
01 Jun 1978

Magnetic Properties of Linear Chain Systems: Metamagnetism of Single Crystal $\text{Co}(\text{pyridine})_2\text{Cl}_2$

Simon N. Foner

Richard B. Frankel

William Michael Reiff

Herbert Wong

et. al. For a complete list of authors, see https://scholarsmine.mst.edu/chem_facwork/2580

Follow this and additional works at: https://scholarsmine.mst.edu/chem_facwork

 Part of the [Chemistry Commons](#)

Recommended Citation

S. N. Foner et al., "Magnetic Properties of Linear Chain Systems: Metamagnetism of Single Crystal $\text{Co}(\text{pyridine})_2\text{Cl}_2$," *Journal of Chemical Physics*, vol. 68, no. 11, pp. 4781-4789, American Institute of Physics (AIP), Jun 1978.

The definitive version is available at <https://doi.org/10.1063/1.435658>

This Article - Journal is brought to you for free and open access by Scholars' Mine. It has been accepted for inclusion in Chemistry Faculty Research & Creative Works by an authorized administrator of Scholars' Mine. This work is protected by U. S. Copyright Law. Unauthorized use including reproduction for redistribution requires the permission of the copyright holder. For more information, please contact scholarsmine@mst.edu.

Magnetic properties of linear chain systems: Metamagnetism of single crystal $\text{Co}(\text{pyridine})_2\text{Cl}_2$

S. Foner and R. B. Frankel

Francis Bitter National Magnet Laboratory, ^{a)} Massachusetts Institute of Technology, Cambridge, Massachusetts 02139

W. M. Reiff^{b)} and H. Wong

Department of Chemistry, Northeastern University, Boston, Massachusetts 02115

Gary J. Long^{c)}

Department of Chemistry, University of Missouri-Rolla, Rolla, Missouri 65401
(Received 3 October 1977)

The metamagnetic behavior of the low temperature properties of single crystal $\text{Co}(\text{pyridine})_2\text{Cl}_2$ is discussed. At 1.25 K oriented single crystals exhibit a two-step metamagnetic transition at applied fields ~ 0.8 and 1.6 kG along the b -axis, a single transition at ~ 0.7 kG for applied fields along the a^* axis, and a single transition at ~ 4.2 kG for an applied field along the c axis. Just above the transition fields a moment of $2\mu_B/\text{Co}$ atom is measured for B_0 parallel to the a^* axis or b axis, and $0.4\mu_B/\text{Co}$ atom is measured for the B_0 parallel to the c axis. A large field dependent moment is observed at high fields. Many features of this compound closely mirror the behavior of $\text{CoCl}_2 \cdot 2\text{H}_2\text{O}$. However, the $\text{Co}(\text{pyridine})_2\text{Cl}_2$ has a much smaller interchain exchange, so that many features can be examined at lower fields. The basic features are consistent with a six-sublattice model for the ordered antiferromagnetic system. Measurements of magnetic moment versus temperature show that $\text{Co}(\text{pyridine})_2\text{Cl}_2$ does not obey a Curie-Weiss law even at relatively high temperatures.

I. INTRODUCTION

There has been considerable recent interest in the electronic and magnetic properties of quasi-one-dimensional magnetochemical systems.¹ These materials are characterized by a large ratio of the intrachain exchange J to the interchain exchange J' ($|J/J'| \gg 1$), and the interaction between spins is taken to be $-2JS_1 \cdot S_2$.

Two general types of antiferromagnetic ordering occur in such systems. In the first the intrachain interaction is negative ($J < 0$) and below the three-dimensional ordering temperature T_N adjacent spins in the chain are aligned antiparallel. In the second the intrachain interaction is positive ($J > 0$) and the interchain interaction is negative ($J' < 0$) and below T_N adjacent spins in the chain are aligned parallel whereas the spins in adjacent chains are aligned antiparallel. In the latter case, when the antiferromagnetic (interchain) exchange field is much smaller than the anisotropy field, an applied field of the order of the exchange field may induce one or more (first-order) magnetic phase transitions, called metamagnetic transitions, to configurations with higher total magnetic moment.

Important examples of quasi-one-dimensional metamagnets include $\text{FeCl}_2 \cdot 2\text{H}_2\text{O}$ and $\text{CoCl}_2 \cdot 2\text{H}_2\text{O}$ with $T_N = 23.5$ and 17.2 K, respectively.²⁻⁶ In both cases the intrachain interaction is positive with antiparallel align-

ment of adjacent chains below T_N . At 4.2 K two metamagnetic transitions are observed for the applied field B_0 parallel to the initial spin direction, at 39 and 45 kG in $\text{FeCl}_2 \cdot 2\text{H}_2\text{O}$, and at 32 and 46 kG in $\text{CoCl}_2 \cdot 2\text{H}_2\text{O}$. Two transitions are observed in each case because of a finite interaction (J'') between chains with the same initial spin orientation. Narath^{2,4} has introduced a six-sublattice model which accounts for the transitions as follows: Initially, the antiferromagnetic state consists of three ferromagnetic chains of Co ions with spins up (abbreviated here as three spins up) and three spins down. The first transition is to a ferromagnetic phase with four spins up and two spins down, and the second transition is to a fully aligned paramagnetic phase. In this model the moment of the ferrimagnetic phase is $1/3$ that of the paramagnetic phase, in agreement with the observed values.

The one-dimensional magnetic character can be enhanced by replacing the transaxial aquo groups by bulkier organic groups such as pyridine. This has the effect of reducing the interchain interaction, and consequently the Néel temperature and the critical fields required for the metamagnetic transitions.

The series of linear chain $\text{M}(\text{pyridine})_2\text{X}_2$ complexes have received the attention of both chemists and physicists from theoretical and experimental points of view.⁷⁻¹² In this series M is a $3d$ transition metal and, X is a halogen such as chlorine or bromine or a pseudo-halogen, e.g., thiocyanate. In the series with X = Cl the copper and manganese complexes have a negative intrachain interaction while the iron, cobalt, and nickel analogues have a positive intrachain interaction and a negative interchain interaction, as in the iron and cobalt halide dihydrates. The one-dimensional magnetic character of the pyridine complexes is especially evident in

^{a)}Supported by the National Science Foundation.

^{b)}Supported by the National Science Foundation Division of Materials Research, Solid State Chemistry Program Grant No. DMR 77-12625A01, and partially by the Research Corp. and H. E. W. Grant No. RR 07143.

^{c)}Supported by the National Science Foundation Division of Physical Sciences, Inorganic and Organometallic Synthesis Program Grant No. CHE-75-20417.

the magnetic heat capacity^{7,8} which often exhibits a broad "one-dimensional" peak or shoulder at temperatures above a sharper λ anomaly that reflects the three-dimensional ordering temperature T_N .

Powder samples of the pyridine systems have been studied by several techniques including measurements of the heat capacity, magnetization, and magnetic susceptibility. The temperature dependence of the magnetic susceptibility of $\text{Co}(\text{pyridine})_2\text{Cl}_2$, measured in low applied fields (0.1 to 40 G), showed¹³ $T_N = 3.17$ K and a paramagnetic Curie temperature $\theta = +5$ K. A theoretical fit of the susceptibility above T_N with a ferromagnetic Ising model yielded an intrachain interaction $J/k = 11.7$ K. Subsequent studies of the powder magnetization¹⁴ below T_N showed a rapidly increasing moment with increasing field, indicative of first order metamagnetic transition at fields of the order of 0.7 kG. Similar transitions were observed in $\text{Fe}(\text{pyridine})_2\text{Cl}_2$, $\text{Ni}(\text{pyridine})_2\text{Cl}_2$, and $\text{Fe}(\text{pyridine})_2(\text{NCS})_2$ at fields of 0.7, 2.7, and 1.1 kG, respectively, at 4.2 K (below T_N in each case). Magnetization measurements up to 60 kG showed that magnetic saturation was not achieved for any of the materials, reflecting high anisotropy.

In order to further elucidate the nature of the metamagnetic transitions and to make more complete comparisons with the metal halide dihydrates we have made magnetic measurements in oriented single crystals of $\text{Co}(\text{pyridine})_2\text{Cl}_2$. Single crystal studies of intrachain antiferromagnetic pyridine compounds, namely, $\text{Mn}(\text{pyridine})_2\text{Cl}_2$ and $\text{Cu}(\text{pyridine})_2\text{Cl}_2$, have been reported.^{10,15,16} Preliminary results on single crystal $\text{Co}(\text{pyridine})_2\text{Cl}_2$ also have been reported.¹⁷

II. CRYSTAL STRUCTURE OF $\text{Co}(\text{pyridine})_2\text{Cl}_2$

The crystal structure of α - $\text{Co}(\text{pyridine})_2\text{Cl}_2$ as well as the isomorphous iron system is monoclinic, space group $C2/b$ at room temperature.^{18,19} Each metal atom of the chain is in a pseudo-octahedral environment of four chlorine bridging atoms and two *trans*-pyridine nitrogen atoms with the linear chain (*c* axis) along the direction of the chlorine bridges. The corresponding cobalt and iron chloride dihydrates are linear chain systems that are quite similar²⁰ to the pyridine complexes in that they have chlorobridging and nearly the same (3.6 to 3.9 Å) intrachain metal-metal distances. On the other hand, the dihydrates have a much smaller interchain metal-metal distance (~ 5.5 Å) as opposed to ~ 8 to 9 Å in the pyridine systems.

A detailed study of the crystal structure of α - and γ - $\text{Co}(\text{pyridine})_2\text{Cl}_2$ was recently made by Clarke and Milledge.^{19,21} They found that in the α phase $a = 34.4$ Å, $b = 17.4$ Å, $c = 3.66$ Å and in the γ phase $a = 17.437$ Å, $b = 8.408$ Å, $c = 3.593$ Å. The γ (low temperature phase) is monoclinic with the a^* axis close to the a axis (within 1°). Surprisingly, the low temperature phase has higher overall symmetry, although the chlorobridging along the c axis is symmetric for the α phase and asymmetric for the γ phase. The symmetry for the γ phase is $P2_1/n(b$ unique) and the transition from the α to the γ phase takes place at approximately 150 K for increasing

temperature, and about 134 K for decreasing temperature.

III. CRYSTAL PREPARATION

A sample of polycrystalline $\text{Co}(\text{pyridine})_2\text{Cl}_2$ was prepared by the standard method.²² Chemical analysis was consistent with this stoichiometry as follows: % analysis calc. for $\text{CoC}_{10}\text{H}_{10}\text{N}_2\text{Cl}_2$: Co, 20.43; C, 41.70; H, 3.50; N, 9.72; found: Co, 20.23; C, 41.54; H, 3.43; N, 9.61. A saturated solution of the compound in absolute ethanol at 50°C was prepared. This solution was blue and indicative of the presence in solution of the tetrahedral β isomer of $\text{Co}(\text{pyridine})_2\text{Cl}_2$. The solution was slowly cooled (in steps of $5^\circ\text{C}/\text{day}$) to room temperature. During this time single crystals of the linear chain octahedral α isomer of $\text{Co}(\text{pyridine})_2\text{Cl}_2$ were formed. A microscopic examination of these crystals indicated that they were dichroic with biaxial interference and possessed the same crystal morphology as the crystals used in a recent single crystal x-ray crystallographic study by Clarke and Milledge.¹⁹ This study confirmed the earlier report¹⁸ that these crystals were twinned at temperatures above ~ 150 K. The twinning probably occurs by reflection across the (100) plane.¹⁹ However, this twinning vanishes at temperatures below the reversible α - to γ -phase transition which occurs at ~ 150 K.^{19,21}

IV. MAGNETIC MOMENT MEASUREMENTS

A. Experimental details

Measurements of the magnetic moment σ as a function of applied field B_0 , temperature T , and crystallographic orientation were made for several single crystal samples of $\text{Co}(\text{pyridine})_2\text{Cl}_2$. The single crystals were mounted on a suitable oriented surface with a very thin layer of silicone grease. The grease permitted orientation of the crystallite with respect to the applied field, and minimized decomposition via the loss of pyridine. Additional measurements were made for polycrystalline pyridine complexes of iron, cobalt, and nickel. Low field measurements were made in a superconducting magnet by using a vibrating sample magnetometer. The

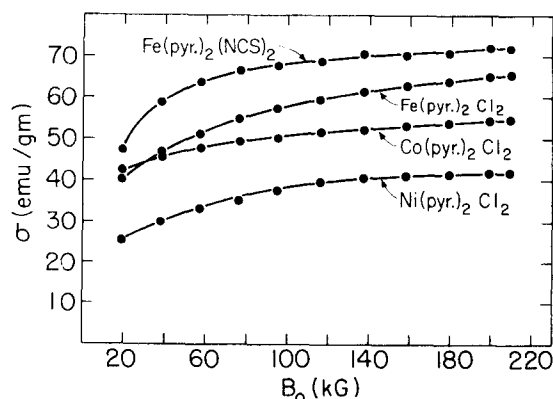


FIG. 1. Magnetic moment σ vs applied field B_0 for several powdered pyridine compounds at 4.2 K. Very low field transitions are observed for $B_0 < 3$ kG for the Ni, Co, and Fe compounds (see Refs. 14 and 23).

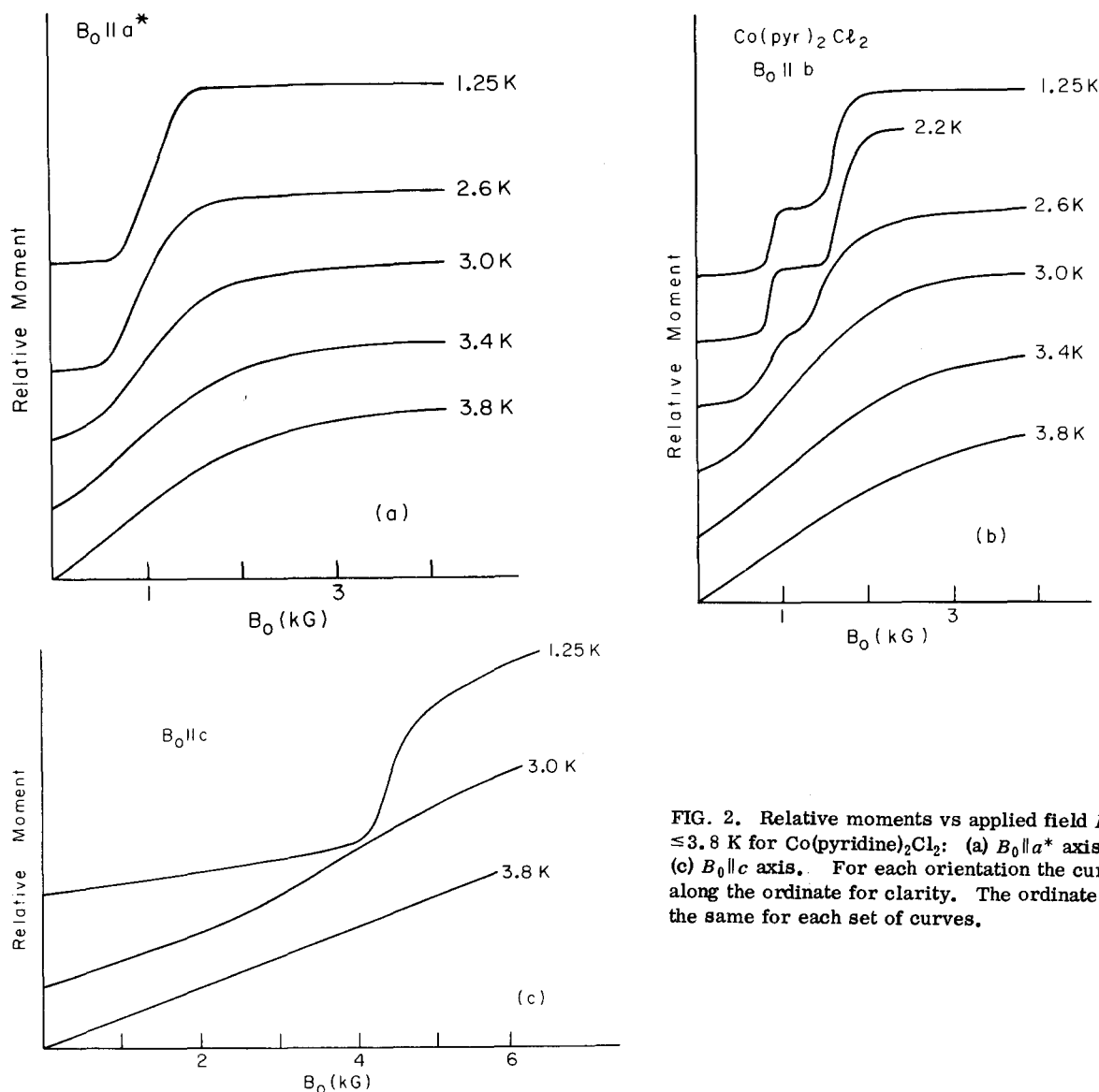


FIG. 2. Relative moments vs applied field B_0 for $1.25 \leq T \leq 3.8$ K for $\text{Co}(\text{pyridine})_2\text{Cl}_2$: (a) $B_0 \parallel a^*$ axis; (b) $B_0 \parallel b$ axis; (c) $B_0 \parallel c$ axis. For each orientation the curves are displaced along the ordinate for clarity. The ordinate scales are not the same for each set of curves.

high-field measurements (above 60 kG) were made on polycrystalline samples by using a low frequency vibrating sample magnetometer operating in a high-power water-cooled Bitter solenoid up to 230 kG. Less direct evidence of metamagnetic transitions in the pyridine complexes was obtained from studies of polycrystalline materials.^{14,23} The details of the magnetic properties of these materials are best understood by examining single crystal data because the transitions are sensitive to the orientation of the applied field with respect to the spin orientation.

B. Powder data

The magnetic characteristics of polycrystalline $\text{M}(\text{pyridine})_2\text{X}_2$, where M is divalent Fe, Co, or Ni and X is Cl or (NCS), have been discussed in Refs. 14 and 23. The low-field differential susceptibility shows a very sharp maximum after which the susceptibility decreases to a small value as T is decreased.^{13,23} In addition, all the materials show relatively large low-field changes in σ vs B_0 for $T < T_N$. After the rapid rise in moment there

is a gradual approach toward saturation in high fields to 200 kG (see Fig. 1). However, saturation is not achieved even at these fields.

C. Single crystal data

1. Low field characteristics

Measurements of single crystals were made on composites of several single crystals or with independent single crystals. Unless otherwise stated the single crystal data is given for composites all weighing a total of a few mg. Often the sample weights are given in the figure captions. Isothermal magnetic moment versus field data along the b , a^* , and c axes are shown in Fig. 2. Evidence of long-range order occurs near 3.2 K, in agreement with the earlier powder sample data.^{9,14} Along the a^* and c axes a single transition is observed, whereas along the b axis, essentially the direction of the *trans*-pyridine nitrogens, there are two steps in the magnetic moment. The characteristics along the b axis are reminiscent of those observed for $\text{CoCl}_2 \cdot 2\text{H}_2\text{O}$ along

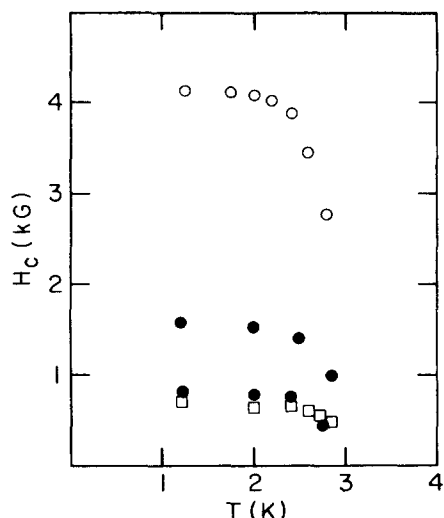


FIG. 3. Transition fields H_c vs T for single crystal $\text{Co}(\text{pyridine})_2\text{Cl}_2$. Squares, $B_0 \parallel a^*$ axis; solid circles, $B_0 \parallel b$ axis; open circles, $B_0 \parallel c$ axis.

the b axis, where two transitions were observed³ at applied fields of 31.6 and 46 kG. An analogous single transition along the c axis of the hydrated salt has not been reported for $\text{CoCl}_2 \cdot 2\text{H}_2\text{O}$. Apparently, the applied fields were too low to permit observation of this transition.

We may define the transition field H_c as that field for which the σ versus B_0 data (in the transition field region) extrapolates to $\sigma=0$ on the B_0 axis, or as the extrapolation of $\sigma(B_0)$ to the linear portion of initial susceptibility. Although the differences in H_c are not large for these two definitions when $\sigma(B_0)$ is nearly vertical, appreciable differences occur when the initial susceptibility is relatively large compared to the change in σ at the transition, and/or when the depolarization factor is large. The largest errors in defining H_c by either procedure occur near T_c , where σ vs B_0 at low fields is large and comparable to σ vs B_0 just above H_c . In the present paper σ vs B_0 is plotted with no depolarizing factor correction. For B_0 along the a^* or b axis the depolarizing factor is quite small because the crystallites are very thin platelets with the large dimension along the c axis. However, the depolarizing factor for B_0 along the c axis is nearly that of a flat plate (4π). The largest errors in defining H_c therefore would occur along the c axis. Defining H_c as the extrapolation of $\sigma(B_0)$ downward to the intersection with the linear portion of the initial susceptibility minimizes the errors and we choose this procedure. The plot of $H_c(T)$ vs T as defined in this manner is shown in Fig. 3 for each axis. The general features are that, for each transition, $H_c(T)$ becomes large and essentially temperature independent below ~ 2 K and decreases very rapidly toward $H_c(T)=0$ near T_c . The values of $H_c(T)$ were determined within an accuracy of about 10% from plots such as those shown in Fig. 2.

At the lowest temperature (1.25 K) the transition along the a^* axis occurs at ~ 700 G, along the b axis at values of 800 and 1500 G, and along the c axis at ~ 4 kG. A small hysteresis of $H_c(T)$ is observed in some cases

for the low-field transition along the b axis. The previous¹⁴ polycrystalline data showed only one transition, which can be understood in terms of broadening introduced by randomly oriented crystallites. The transitions along a^* and b axes occur at nearly the same field and the second transition for the b axis occurs over a relatively narrow angular orientation. The moment changes along the b axis for each of the transitions are not equal, the lowest-field step being equal (within a few percent) to 1/2 the change in magnetization for the higher-field transition. It should be noted that, for the measurements presented here, the crystallites were cooled only once for a series of measurements vs B_0 and T . Subsequent measurements for a given orientation were made on new batches of crystallites that were thermally cycled only once. In addition, measurements were made on one single crystal of the order of 0.5 mg weight in order to ensure that the crystal composite was representative of single crystal behavior. In some measurements repeated coolings were made with the same crystals; after several coolings the low-field characteristics along the b axis changed, so that the magnitude of the moment changes became equal for the low-field and high-field transitions. This suggests that the crystal structure is changed. The crystals are sensitive to cooling and handling and tend to shatter in the course of the α to γ transition.¹⁹

Metamagnetism and hysteresis has been discussed²⁴ for FeCl_2 and the features of the magnetic ordering on FeBr_2 , CoBr_2 , FeCl_2 , and CoCl_2 have been examined by neutron scattering.²⁵ The neutron data showed that hysteresis in the magnetic moment at low fields resulted from a change in the three equivalent domain distributions which initially were equally populated, but were not equally populated after the field was applied and returned to zero. In the case of the $\text{CoCl}_2 \cdot 2\text{H}_2\text{O}$ and $\text{FeCl}_2 \cdot 2\text{H}_2\text{O}$ additional hysteresis effects have been reported.^{26,27} Relaxation phenomena associated with the field region between the two H_c 's for B_0 along the b axis in $\text{CoCl}_2 \cdot 2\text{H}_2\text{O}$ were studied with ac modulation techniques.²⁶ Several small jumps in σ vs B_0 were observed

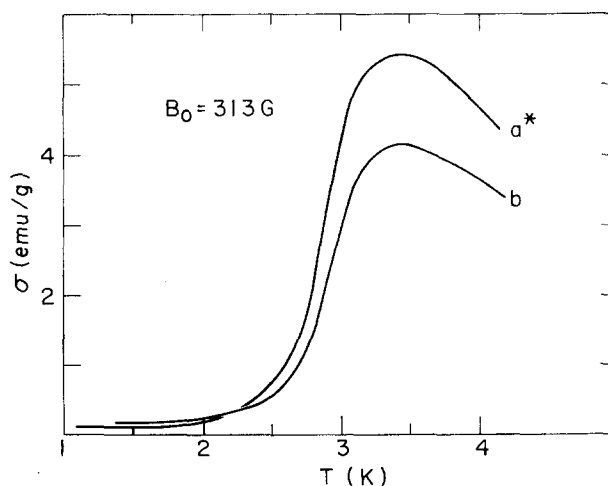


FIG. 4. Moment σ vs T for $B_0=313$ G parallel to the a^* axis and the b axis.

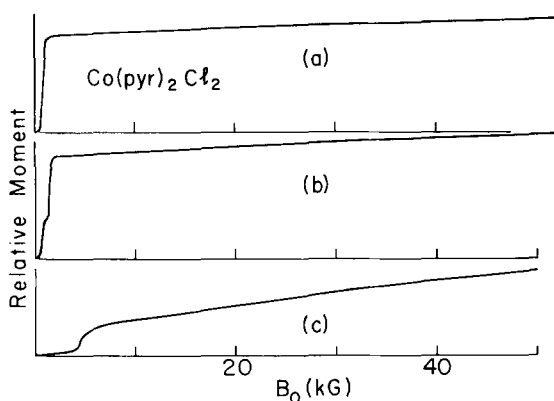


FIG. 5. Relative magnetic moment σ vs applied field B_0 at 1.25 K: (a) $B_0 \parallel a^*$ axis (2.08 mg); (b) $B_0 \parallel b$ axis (2.53 mg); (c) $B_0 \parallel c$ axis (1.88 mg). The moments at $B_0 = 52$ kG are $\sim 2.5 \mu_B/\text{Co}$ atom for (a) and (b), and $\sim 1.1 \mu_B/\text{Co}$ atom for (c).

between the two H_c 's; the relaxation effects were dependent on temperature, frequency, and whether B_0 was increasing or decreasing. Measurements of $\sigma(B_0)$ in $\text{FeCl}_2 \cdot 2\text{H}_2\text{O}$ were reported for pulsed and static fields²⁷ applied along the initial spin direction. Although the high field transition showed no hysteresis, the transition at low field did show varied effects. At 4.2 K the $\sigma(B_0)$ data suggested a six-sublattice model, whereas at lowest temperatures the data were consistent with a four-sublattice model. A large activation energy between the two magnetic states was indicated. Our results for $\text{Co}(\text{pyridine})_2\text{Cl}_2$ do not show these large hysteresis effects down to 1.4 K.

In Fig. 4 we show behavior of the magnetic moment as a function of temperature for an applied field of 313 G along the a^* and b axes for $\text{Co}(\text{pyridine})_2\text{Cl}_2$. The moment along the c axis at $T \sim 4.2$ K and 313 G is about a tenth of that along the a^* axis. The data were taken as each composite sample was cooled slowly in a liquid helium bath and represents ~ 500 points over a single run. Depending on the definition of the transition temperature as either the maximum $d\sigma/dT$ or the maximum in the σ vs T , we obtain a transition temperature of 3.2 to 3.4 K, respectively. The results are in good agreement with the polycrystalline data reported earlier.^{9,14,23} Because H_c is very small, it is possible that a B_0 of 313 G would shift T_N slightly. We have re-examined the magnetic moment σ vs B_0 data at very low fields extrapolating the data to $B_0 = 0$. The initial susceptibility χ_i for each direction as a function of temperature for $0 \leq B_0 \leq 50$ G is qualitatively quite similar to the 313 G data. However, the moments along the a^* and b axes are smaller relative to that along the c axis and the rapid rise near T_N is sharper. The maximum $d\sigma/dT$ occurs at ~ 3.2 K and the maximum in σ occurs at ~ 3.4 K. The value of T_N for the data along the a^* , b , and c axes are consistent (within 0.2 K) and agree with the determination of T_N given earlier for the $\text{Co}(\text{pyridine})_2\text{Cl}_2$ single crystal and polycrystalline data.

All the data for the initial susceptibility χ_i show a rapid drop as T is decreased below T_N . However, for $T < T_N$, $\chi_i(a^* \text{ axis}) < \chi_i(b \text{ axis}) \ll \chi_i(c \text{ axis})$ whereas for $T > T_N$, $\chi_i(a^* \text{ axis}) > \chi_i(b \text{ axis}) \gg \chi_i(c \text{ axis})$. For com-

parison we note that the hydrated salt shows that $\chi(a^* \text{ axis}) \approx \chi(c \text{ axis}) \gg \chi(b \text{ axis})$ for $T \ll T_N$ and $\chi(a^* \text{ axis}) \approx \chi(c \text{ axis}) \ll \chi(b \text{ axis})$ for $T > T_N$. It is interesting that for the pyridine complex the H_c along the c axis is much higher than that along the b axis. $\text{CoCl}_2 \cdot 2\text{H}_2\text{O}$ mirrors several of the magnetic properties of the pyridine complex, but the transitions occur at much higher magnetic fields because the hydrated complex has larger exchange interactions. There are some differences between the results. For instance, in $\text{CoCl}_2 \cdot 2\text{H}_2\text{O}$ H_c along the a^* axis is apparently larger than along the b axis, whereas the reverse is observed for the pyridine complex. We expect that the hydrated complex should show a high field transition along the c axis; this aspect is being investigated.

2. High field characteristics

The magnetic properties for B_0 up to ~ 55 kG and low temperatures are illustrated in Fig. 5. Each set of data is taken for a composite of three oriented crystals. The total weight of each sample is given in the figure caption. The general features are that the large changes in σ occur at very low fields, and there is a gradual increase in magnetic moment at higher fields. In addition, the moment along the c axis is quite small compared to that along the a^* and b axes. The values of the moment at 52 kG are approximately $2.5 \mu_B/\text{Co}$ atom for both the a^* and b axes and approximately $1.1 \mu_B/\text{Co}$ atom along the c axis. For spin only a maximum of $3 \mu_B/\text{Co}$ atom is expected. The moment observed earlier for powder data is consistent with the single crystal results reported here; an average of σ for $B_0 = 50$ kG along the a^* , b , and c axes corresponds to that for the polycrystalline data at the same field. The effects of crystalline electric fields on the Co ion are appreciable so that the spin-only value is not realized. Some of these effects are discussed in Sec. V.

3. Temperature dependence of σ

We also have studied the temperature dependence of σ up to $T \sim 280$ K for the three principal crystallographic directions. The results are complicated by several factors. The α - to γ -phase transition at approximately 150 K produces a change in the magnetic moment which is observable at high resolution. Bentley

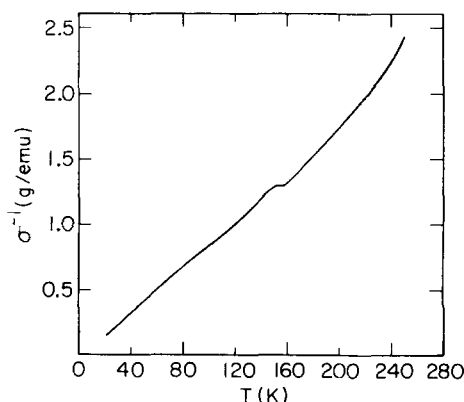


FIG. 6. Inverse moment σ^{-1} vs T for $B_0 = 11.0$ kG along the b axis. The sample is a composite of oriented single crystals with a total weight of 3.8 mg.

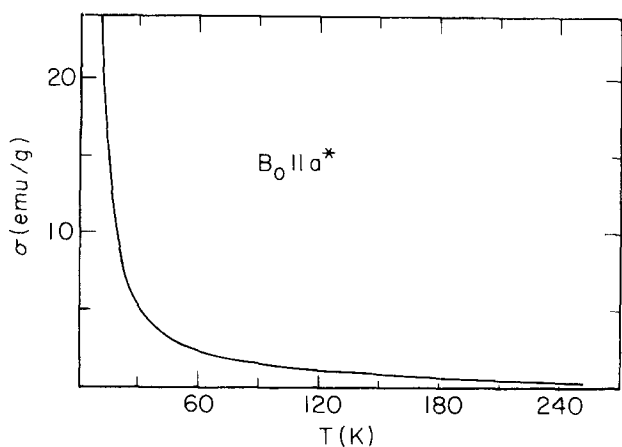


FIG. 7. Moment σ vs T for an applied field $B_0 = 11$ kG along the a^* axis. The sample is a composite of oriented single crystals with a total weight of 6.2 mg.

*et al.*²⁸ examined the differential susceptibility for powders and single crystal material at high T (from 80 to 300 K) by using small crystallites and torsion measurements and observed small steps in moment near the α -to- γ -transformation temperature. Our attempts to fit the published data of Bentley *et al.* with a Curie-Weiss law were not successful; the value of θ and C , where $\chi = C/(T + \theta)$, depended on the range of T employed in fitting the data. Similar difficulties were encountered in attempting to fit our single crystal results at high T to a Curie-Weiss law. Furthermore, our data below the α to γ transition could not be fit to the Curie-Weiss law for any principal direction. For this reason it was not possible to obtain g values for the data at low T . (In addition to the effects of the crystallographic phase transition, one-dimensional effects, etc., the crystalline electric field contributions to χ would be expected to preclude a Curie-Weiss law.) A plot of σ^{-1} vs T for $B_0 \parallel b$ axis of a 3.8 mg composite of oriented crystals is shown in Fig. 6. The general features show a nonlinear behavior of σ^{-1} vs T over the entire range of T . Below the α to γ transition $d(\sigma^{-1})/dT$ is nonlinear and above the transformation it increases with increasing T . Here we plot σ^{-1} vs T , rather than χ^{-1} vs T , because σ vs B_0 becomes nonlinear as T approaches the lower temperatures. Clearly, at 4.2 K there is a strong field dependence of σ vs B_0 and data near 4.2 K should reflect this additional feature. In typical antiferromagnetic systems data above $10T_N$ (here ~ 35 K) usually allows one to determine θ from the Curie-Weiss law without recourse to power-series expansion techniques. Although the nonlinear behavior of σ^{-1} vs T above 40 K may reflect contributions of the one-dimensional behavior of this magnetic structure as well as the influence of the α to γ transformation at higher T , the rather complex behavior indicates that Curie-Weiss fits are not appropriate. These results suggest that magnetic moment measurements of similar linear chain type systems, made in order to determine g values and/or exchange interactions, should be made over an extended range of temperatures in order to assure that the assumption of a Curie-Weiss law is valid. In addition, $\sigma(T)$ increases very rapidly as the temperature is reduced toward the

ordering temperature and is strongly field dependent. Typical σ vs T results are shown in Fig. 7 for $B_0 = 11$ kG. The plot is based on ~ 1000 points (which are not shown for convenience). Bentley *et al.* observed $\chi_a > \chi_b$ for $T < 140$ K (in agreement with our low- T data) and $\chi_a < \chi_b$ above ~ 160 K (the α -to- γ -transition region). They also indicate that the moment changes are quite small ($\sim 2\%$) at the α to γ transition, but that the changes in anisotropy would have significant effects on the magnetic properties. We also have observed small moment changes $\sim 2\%$ at the α to γ transition for B_0 along, for example, the a^* axis and b axis for single crystal composites. This would be visible in the data such as that of Fig. 7 when expanded sufficiently. The plot of σ^{-1} vs T in Fig. 6 for $B_0 \parallel b$ axis shows this clearly. Although the data are qualitatively in agreement with those of Bentley *et al.*, the signal-to-noise ratio was not sufficient for detailed quantitative results, particularly in view of the effects on the structure produced by cycling through the α to γ transition.

V. DISCUSSION OF RESULTS

A. Magnetic structure of $\text{Co}(\text{pyridine})_2\text{Cl}_2$

The local arrangements of atoms in the neighborhood of the Co ion is shown in Fig. 8. The Co is surrounded by four Cl ions which make angles close to, but different from, 90° . In contrast to the high-temperature α phase, the Co-Cl distances between the chlorine atoms in the γ phase are not identical and the structure is very similar to that of the $\text{Cu}(\text{pyridine})_2\text{Cl}_2$.

The moment changes of $(2/3)\mu_B$ and $(4/3)\mu_B/\text{Co}$ atom at fields of 0.8 and 1.6 kG, respectively, applied along the b axis are analogous to the transitions observed at higher fields along the b axis of $\text{CoCl}_2 \cdot 2\text{H}_2\text{O}$. This, together with the low field susceptibility data at high and low temperature, suggest a magnetic structure similar to that proposed by Narath for $\text{CoCl}_2 \cdot 2\text{H}_2\text{O}$, as shown in Fig. 9. In this case we assume that the spins are along the b axis with the relevant exchange interactions as shown. J_0 is the dominant (ferromagnetic) exchange along the chain (c axis), J_1 is the nearest-neighbor interchain antiferromagnetic exchange, and J_2 and J_3 are

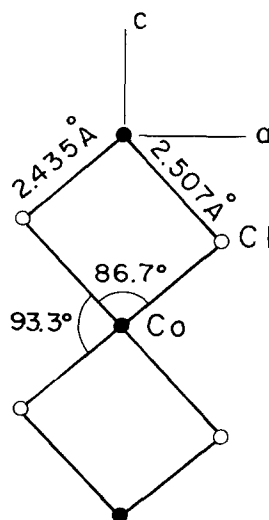


FIG. 8. Local arrangement of atoms at Co site for γ - $\text{Co}(\text{pyridine})_2\text{Cl}_2$.

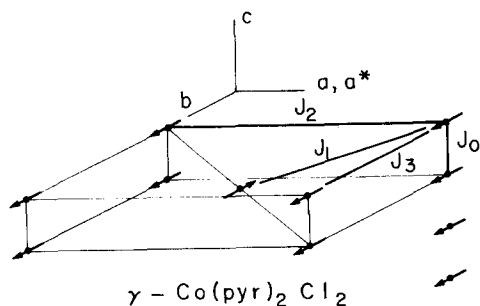


FIG. 9. Suggested spin arrangement for the $\gamma\text{-Co}(\text{pyridine})_2\text{Cl}_2$ structure showing ferromagnetic exchange J_0 between atoms along c -axis chain, interchain antiferromagnetic interactions J_1 , and interchain interactions J_2 and J_3 .

next-neighbor ferromagnetic exchange interactions. Close examination of the structure shows another relatively short exchange path J_4 (not shown in Fig. 9) between the Co atom at the body center position and the next lower or upper Co atom (visualized by tipping J_2 up or down one lattice spacing along the c axis). The exchange interaction, relevant Co-Co intrinsic distances, and number of exchange paths are tabulated in Table I.

The relative moment change of 1:2 for the two transitions is accounted for by a six-sublattice model, with three up and three down spins. In the first transition ($B_0 = 0.8$ kG) one down spin reorients up, and at the second transition ($B_0 = 1.6$ kG) the remaining two down spins reorient up, giving the 1:2 relative moment change. For a four-sublattice model the relative moment change would be 1:1. If there were two sublattices, only a single metamagnetic transition for saturation would be observed. There is evidence in $\text{CoCl}_2 \cdot 2\text{H}_2\text{O}$ that either a four- or six-sublattice model is appropriate depending on the manner in which the transitions are approached (see Sec. IV.C1). As we mentioned earlier, when some of the $\text{Co}(\text{pyridine})_2\text{Cl}_2$ crystals were cooled several times, a transformation from the six-sublattice to four-sublattice behavior was noted. There is no evidence in the σ vs B_0 data for canting of the antiferromagnetically aligned spins as is observed in $[(\text{CH}_3)_3\text{NH}][\text{CoCl}_3 \cdot 2\text{H}_2\text{O}]$, which also consists essentially of $\text{CoCl}_2 \cdot 2\text{H}_2\text{O}$ chains with ferromagnetic exchange along the chain.²⁹⁻³¹

The suggested spin structure with spins parallel to the b axis is consistent with the magnetic susceptibility data which shows that at lowest temperature $\chi(b$ axis) is less than $\chi(a^*$ axis). Data for $\text{CoCl}_2 \cdot 2\text{H}_2\text{O}$ also shows that $\chi(b$ axis) is the lowest at low temperature,

TABLE I. Exchange interactions J_i relevant Co-Co internal distances and number of exchange paths for $\gamma\text{-Co}(\text{pyridine})_2\text{Cl}_2$.

No. of paths and zero field interaction	Symbol	Co-Co distance (\AA)
2F	J_0	3.59
8AF	J_1	9.83
2F	J_2	17.4
2F	J_3	8.41
4F	J_4	9.16

F = ferromagnetic; AF = antiferromagnetic.

and independent microscopic measurements^{3,4} have confirmed that the moments are oriented along the b axis. The very small observed transition fields for the metamagnetic transitions indicates that the exchange interactions are extremely small so that they are overcome by relatively weak applied fields. Thus, although we expect J_0 to be similar for $\text{CoCl}_2 \cdot 2\text{H}_2\text{O}$ and $\text{Co}(\text{pyridine})_2\text{Cl}_2$, J_1 is observed to be much smaller for the $\text{Co}(\text{pyridine})_2\text{Cl}_2$.

In a manner similar to that used by Narath,^{3,32} we can solve for the magnitude of J_1 and J_2 based on the measured values of H_c at 1.4 K along the b axis assuming that $|J_3| \ll |J_2|$. We have

$$H_{c1} = (g_b \mu_B)^{-1} \sigma (-2J_1 Z_1 + 4J_2 Z_2)$$

$$H_{c2} = (g_b \mu_B)^{-1} \sigma (-2J_1 Z_1 - 2J_2 Z_2)$$

if $Z_1 = 4$ and $Z_2 = 2$ are chosen as the number of interchain neighbors. Although g_b is not evaluated, the ratio J_1/J_2 is obtained from the measured values of H_{c1} and H_{c2} . In this case we find $J_1/J_2 \approx 2.5$ for H_c of 800 and 1600 G for the two transition fields. The corresponding value for $\text{CoCl}_2 \cdot 2\text{H}_2\text{O}$ is $J_1/J_2 \approx 4.2$. [For $Z_1 = 8$, $J_1/J_2 \approx 1.25$ in $\text{Co}(\text{pyridine})_2\text{Cl}_2$.] The choice of J_2 and J_3 in Fig. 9 assumes $|J_2| \gg |J_3|$. If $|J_2| \ll |J_3|$, the same results are achieved with this model if J_2 and J_3 are interchanged in Fig. 9. As discussed by Narath,² a four-sublattice structure should be observed if $J_3 < 0$, so that the six-sublattice structure suggests that $J_3 \gtrsim 0$. The observation of two equal steps in magnetization after repeated cycling (Sec. IV.C.1) suggests a change in sign (or magnitude) of J_3 caused by a change in structure.

We must also account for the single transitions along the a^* and c axes observed in the present case which are not observed in $\text{CoCl}_2 \cdot 2\text{H}_2\text{O}$. The transition along the a^* axis at 0.7 kG is especially interesting. The moment change of $2\mu_B/\text{Co}$ atom is, within experimental error, equal to the resultant moment following the two transitions along the b axis.³¹

By using the model of Fig. 9 the field applied along the a^* axis causes all the spins to reorient simultaneously to a parallel configuration along a^* which is perpendicular to their original orientation along b . The magnitudes of the transition fields for a^* and b and the resultant moments are consistent with the observation that $\chi_a \approx \chi_b$ both above and below T_N . In this respect $\text{Co}(\text{pyridine})_2\text{Cl}_2$ is significantly different from $\text{CoCl}_2 \cdot 2\text{H}_2\text{O}$, for which $\chi_b \gg \chi_a$ and χ_c . The transition along the c axis at $B_0 \approx 4$ kG with a resultant moment of $0.4 \mu_B/\text{Co}$ atom reflects the fact that $\chi_c \ll \chi_a$ and χ_b .

The lack of magnetic saturation of $\text{Co}(\text{pyridine})_2\text{Cl}_2$ at very high field is initially somewhat surprising. In the range of 50 kG (the susceptibility is quite large, however, for fields between 100 and 200 kG) the high field susceptibility becomes relatively small and as pointed out to us by Jacobs (private communication), the high-field moment change would be consistent with estimates of Van Vleck susceptibilities for the Fe^{2+} or Co^{2+} ion.^{24,33} We do not have quantitative measures of the crystalline electric field contributions for the $\text{Co}(\text{pyridine})_2\text{Cl}_2$ system at this time. These contributions differ greatly

for Co^{2+} in various local environments. The α and γ phases have different local symmetry and it is not yet clear which phase is being observed at low temperature.³¹ Some significant differences in the low-field χ data observed by Narath for $\text{CoCl}_2 \cdot 2\text{H}_2\text{O}$ were mentioned above. In addition, the saturation moment just above the metamagnetic transition of this compound² was $\approx 3\mu_B/\text{Co}$ ion; this moment is well above that observed for the $\text{Co}(\text{pyridine})_2\text{Cl}_2$. Attempts to fit the high temperature data of $\text{Co}(\text{pyridine})_2\text{Cl}_2$ in the α phase including crystalline electric fields have been made.³⁴

VI. CONCLUSION

The primary effect of dilution by axial organic groups such as pyridine is to decrease the interchain interaction, and thus the Néel temperature as well as the critical fields required for metamagnetic transitions. Anhydrous ferrous chloride (CdCl_2 structure) has layers of iron atoms with antiferromagnetic interlayer interactions via superexchange through axial chloride anions. It orders antiferromagnetically at ~ 23 K, and at 4.2 K undergoes a single step metamagnetic transition²⁵ to a paramagnetic state for an applied field of ~ 11 kG. As mentioned previously, the linear chain dihydrates $\text{FeCl}_2 \cdot 2\text{H}_2\text{O}$ and $\text{CoCl}_2 \cdot 2\text{H}_2\text{O}$ ($T_N = 23.5$ and 17.2 K, respectively) are intrachain ferromagnetic and characterized by a two step metamagnetism, antiferro- to ferromagnetic and ferrimagnetic to paramagnetic at 39 and 45 kG and 32 and 46 kG, respectively.²⁻⁸ As we have seen above, replacement of the water by pyridine reduces the critical fields for the metamagnetic transitions to the order of 1 kG.

Pyridine closely approximates an "ideal" ligand for producing one-dimensional magnetic systems because of the absence of strong hydrogen bonding interactions which are present in the hydrates. For example, $\text{MnCl}_2 \cdot 2\text{H}_2\text{O}$ is an antiferromagnet ($T_N = \sim 6.9$ K) with nearly equal intra- and interchain exchange.³⁵ The easy axis is along the *trans*- H_2O direction (*b* axis) and superexchange via hydrogen bonding is apparently important. The use of axial ligands bulkier than pyridine might reduce the interchain interactions even more and enhance the one-dimensional magnetic character. This would suppress the Néel temperature and be desirable for the comparison of the magnetic properties of ferromagnetic chains with theory. The transition fields would also be reduced. Variation of the intrachain exchange interaction through the use of other bridging ligands in place of Cl along the chemical chain would also be of interest.

The $\text{Co}(\text{pyridine})_2\text{Cl}_2$ system would appear to be an interesting system for studies in the region of the tricritical point. The value of $T_c \approx 3.2$ K is in an easily accessible range of temperature. However, the difficulty in developing large single crystals and in retaining a single known phase at low temperatures create some problems. Because the $\text{Co}(\text{pyridine})_2\text{Cl}_2$ system is an even better approximation to an ideal linear chain system than $\text{Co}(\text{H}_2\text{O})_2\text{Cl}_2$, such studies would be interesting. As indicated in Fig. 1, there are many $\text{M}(\text{pyridine})_2\text{X}_2$ which undergo metamagnetic transitions at low fields. If single crystals are available, this class of compounds

would furnish a variety of model systems for studies of critical phenomena.

- ¹L. J. DeJongh and A. R. Miedema, *Adv. Phys.* **23**, 1 (1974).
- ²A. Narath, *Phys. Rev. Sect. A* **139**, 1221 (1965).
- ³A. Narath, *J. Phys. Soc. Jpn.* **19**, 2244 (1964); *Phys. Rev. Sect. A* **136**, 766 (1964).
- ⁴D. E. Cox, G. Shirane, B. C. Frazer, and A. Narath, *J. Appl. Phys.* **37**, 1126 (1966).
- ⁵H. Weitzel and W. Schneider, *Solid State Commun.* **14**, 1025 (1974).
- ⁶L. Kandel, M. A. Weber, R. B. Frankel, and C. R. Abeledo, *Phys. Lett. A* **46**, 369 (1974).
- ⁷M. Steiner, J. Villain, and G. G. Windsor, *Adv. Phys.* **25**, 87 (1976).
- ⁸F. W. Klaaijzen, Z. Dokoupil, and W. J. Huiskamp, *Physica (Utrecht)* **79**, 545 (1975), and references cited therein.
- ⁹G. J. Long, D. L. Whitney, and J. E. Kennedy, *Inorg. Chem.* **10**, 1406 (1971).
- ¹⁰P. M. Richards, R. K. Quinn, and B. Morosin, *J. Chem. Phys.* **59**, 4474 (1973).
- ¹¹W. Duffy, Jr., J. E. Venneman, D. L. Strandburg, and P. M. Richards, *Phys. Rev. B* **9**, 2220 (1974).
- ¹²H. T. Witteveen, W. L. C. Rutten, and J. Reedijk, *J. Inorg. Nucl. Chem.* **37**, 913 (1975).
- ¹³K. Takeda, S. Matsukawa, and T. Haseda, *J. Phys. Soc. Jpn.* **30**, 1330 (1971).
- ¹⁴S. Foner, R. B. Frankel, W. M. Reiff, B. F. Little, and G. J. Long, *Solid State Commun.* **16**, 159 (1975).
- ¹⁵Y. Endoh, G. Shirane, R. J. Birgenau, P. M. Richards, and S. L. Holt, *Phys. Rev. Lett.* **32**, 170 (1974).
- ¹⁶K. Andres, S. Darack, and S. L. Holt, *Solid State Commun.* **15**, 1087 (1974).
- ¹⁷S. Foner, R. B. Frankel, W. M. Reiff, H. Wong, and G. J. Long, *AIP Conf. Proc.* **29**, 510 (1976).
- ¹⁸J. Dunitz, *Acta Crystallogr.* **10**, 207 (1957).
- ¹⁹P. J. Clark and H. J. Milledge, *Acta Crystallogr. Sect. B* **31**, 1543 (1975).
- ²⁰D. Harker, *Z. Kristallogr.* **93**, 136 (1976).
- ²¹P. J. Clarke and H. J. Milledge, *Acta Crystallogr. Sect. B* **31**, 1554 (1975).
- ²²N. S. Gill and R. S. Nyholm, *J. Inorg. Nucl. Chem.* **18**, 88 (1961).
- ²³S. Foner, R. B. Frankel, E. J. McNiff, Jr., W. M. Reiff, B. F. Little, and G. J. Long, *AIP Conf. Proc.* **24**, 363 (1975).
- ²⁴T. S. Jacobs and P. E. Lawrence, *Phys. Rev.* **164**, 869 (1967).
- ²⁵M. K. Wilkinson, J. W. Cable, E. O. Wollan, and W. C. Koehler, *Phys. Rev.* **113**, 497 (1959).
- ²⁶Y. Kuramitsu, K. Amaya, and T. Haseda, *J. Phys. Soc. Jpn.* **33**, 83 (1972).
- ²⁷K. Katsumata, *J. Phys. Soc. Jpn.* **39**, 42 (1975).
- ²⁸R. B. Bentley, M. Gerloch, J. Lewis, and P. N. Quedstedt, *J. Chem. Soc. A* **1971**, 375.
- ²⁹D. B. Losee, J. N. McElearney, G. E. Shankle, R. L. Carlin, P. J. Cresswell, and W. T. Robinson, *Phys. Rev. B* **8**, 2185 (1973).
- ³⁰R. D. Spence and A. C. Botterman, *Phys. Rev. B* **9**, 2993 (1974).
- ³¹A very recent paper, W. J. M. de Jonge, Q. A. G. van Vimmeren, J. P. A. M. Hijmans, C. H. W. Swüste, J. A. H. M. Buys, and G. J. M. van Workum, *J. Chem. Phys.* **67**, 751 (1977) presents NMR data which suggest an alternate model in which the antiparallel spin alignment is at an angle of approximately 45° to the a^* and b axes. The authors also suggest that their $\text{Co}(\text{pyridine})_2\text{Cl}_2$ crystals are in the α phase (rather than the γ phase), and show data to

~ 3 kG ($\sigma_b \approx 2.0 \mu_B/\text{Co}$ atom along the axis). We do not have microscopic data; however, the observation of the small moment change at high temperatures (see Fig. 7 and Ref. 28) where the α - γ transition occurs suggests that we are observing the γ phase. Reported twinning and ease of fracture of these crystals indicates that it may be difficult to unambiguously determine the spin structure until the crystallographic transformations of crystals can be controlled.

³²A. Narath, *Phys. Lett.* **13**, 12 (1964).

³³I. S. Jacobs and P. E. Lawrence, *J. Appl. Phys.* **35**, 996 (1964); I. S. Jacobs, P. E. Lawrence, and S. D. Silverstein, *Bull. Am. Phys. Soc.* **10**, 351 (1965); S. D. Silverstein, and I. S. Jacobs, *Phys. Rev. Lett.* **12**, 670 (1964).

³⁴See Ref. 28 and references cited therein. Calculations of crystalline electric field effects for CoCl_2 are discussed by M. E. Lines, *Phys. Rev.* **131**, 546 (1963).

³⁵J. N. McElearney, S. Merchant and R. L. Carlin, *Inorg. Chem.* **12**, 906 (1973).